Journal of Advanced Research 24 (2020) 475–483

Contents lists available at ScienceDirect

Journal of Advanced Research

journal homepage: www.elsevier.com/locate/jare

Bioprospecting a native silver-resistant *Bacillus safensis* strain for green synthesis and subsequent antibacterial and anticancer activities of silver nanoparticles

Temoor Ahmed [a,b], Muhammad Shahid [a,*], Muhammad Noman [a,b], Muhammad Bilal Khan Niazi [c], Muhammad Zubair [a], Ahmad Almatroudi [d], Mohsin Khurshid [e], Farheen Tariq [f], Rabia Mumtaz [a], Bin Li [b]

[a] *Department of Bioinformatics and Biotechnology, Government College University, Faisalabad 38000, Pakistan*
[b] *State Key Laboratory of Rice Biology and Ministry of Agriculture Key Laboratory of Molecular Biology of Crop Pathogens and Insects, Institute of Biotechnology, Zhejiang University, 310058 Hangzhou, China*
[c] *School of Chemical and Materials Engineering (SCME), National University of Sciences & Technology (NUST), Sector H-12, Islamabad 44000, Pakistan*
[d] *Department of Medical Laboratories, College of Applied Medical Sciences, Qassim University, Buraydah, Saudi Arabia*
[e] *Department of Microbiology, Government College University, Faisalabad 38000, Pakistan*
[f] *The Second Affiliated Hospital of Xi'an Jiaotong University, Xi'an 710004, Shaanxi, PR China*

HIGHLIGHTS

- Taxonomic identification of a native silver-resistant bacterial strain.
- Synthesis of silver nanoparticles (AgNPs) by the green method.
- Characterization of purified AgNPs by spectroscopic and imaging techniques.
- Measurement of antibacterial activity of AgNPs against human pathogens.
- Estimation of anticancer potential of AgNPs against liver cancer cell line.

GRAPHICAL ABSTRACT

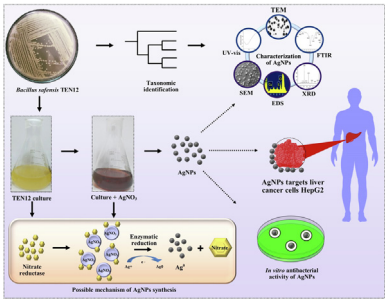

ARTICLE INFO

Article history:
Received 29 February 2020
Revised 16 April 2020
Accepted 7 May 2020
Available online 17 May 2020

Keywords:
AgNPs
Anticancer activity
Antimicrobial activity
B. safensis
HepG2
HEK293

ABSTRACT

Green nanomaterials have gained much attention due to their potential use as therapeutic agents. The present study investigated the production of silver nanoparticles (AgNPs) from a silver-resistant *Bacillus safensis* TEN12 strain, which was isolated from metal contaminated soil and taxonomically identified through 16S rRNA gene sequencing. The formation of AgNPs in bacterial culture was confirmed by using UV–vis spectroscopy with an absorption peak at 426.18 nm. Fourier transform infrared (FTIR) spectroscopy confirmed the involvement of capping proteins and alcohols for stabilization of AgNPs. Moreover, X-ray diffraction analysis (XRD), scanning and transmission electron microscopy (SEM and TEM) confirmed the crystalline nature and spherical shape of AgNPs with particle size ranging from 22.77 to 45.98 nm. The energy dispersive X-ray spectroscopy (EDX) revealed that 93.54% silver content is present in the nano-powder. AgNPs showed maximum antibacterial activity (20.35 mm and 19.69 mm inhibition zones) at 20 μg mL^{-1} concentration against *Staphylococcus aureus* and *Escherichia coli*, respectively and significantly reduced the pathogen density in broth culture. Furthermore, AgNPs demonstrated significant anticancer effects in the human liver cancer cell line (HepG2) in MTT assay, whereas, no cytotoxic effects were demonstrated by AgNPs on normal cell line (HEK293). The present

Peer review under responsibility of Cairo University.
* Corresponding author.
E-mail address: mshahid@gcuf.edu.pk (M. Shahid).

https://doi.org/10.1016/j.jare.2020.05.011
2090-1232/

study suggests that the biogenic AgNPs may substitute chemically synthesized drugs with wider applications as antibacterial and anticancer agents.

Introduction

Pathogenic microorganisms and cancer are major causes of human fatality worldwide. Developing resistance to commercial antibiotics is another dilemma associated with most human pathogens [1]. *Staphylococcus aureus* is a gram-positive bacterium and a member of the normal microbiota in the human body, however, it is one of the most important pathogenic bacteria, acting on a wide range of infections [2]. *S. aureus* leads to a wide spectrum of diseases such as skin and soft tissue infections (SSTIs), osteoarticular infections, endocarditis, sepsis and pneumonia [3,4]. The pathogen synthesizes a number of enzymes and toxins, with positive coagulase being the best known and often implicated in the etiology of a series of infections and poisonings in humans [5]. On the other hand, the *Escherichia coli* is a gram-negative, rod-shaped bacterium and causes bloody diarrhea in humans. Ingestion of food contaminated by *E. coli* leads to gastroenteritis of varying severity, including symptoms such as fever, meningitis, sepsis, and urinary tract infection, etc. [6,7]. Therefore, the effective control of these pathogenic bacteria with novel antibacterial agents is highly desirable [8].

Similarly, cancer is also a leading cause of disease-related mortality and is characterized by an abnormal growth of cells and tissues [9]. Cancer remains one of the world's devastating diseases and its treatment includes radiation, surgery, chemotherapeutic drugs, all of these often killing the healthy cells and causing toxicity to humans. Hepatocellular carcinoma (HCC) is one of the most common types of primary liver cancer, which accounts for approximately 70% of the cases [10,11]. The number of patients of HCC is increasing steadily during the past few decades and it is becoming one of the major reasons for cancer-related deaths. It is highly likely that incidents and deaths associated with HCC will increase in the future. Moreover, exploring the possible reasons and treatments of liver cancer has always been a challenge for scientists and researchers [12]. Imaging and targeted drug delivery using nanomaterials are promising nanotechnology-based approaches in anticancer research [13]. Hence, the anticancer activity of nanoparticles is under the investigation of laboratory-scale to pilot-scale experimentation [14].

In the past few decades, nanotechnology is an emerging area with potential applications in various areas of life sciences including biomedical applications [15]. Metallic nanoparticles (NPs) have countless applications in several fields such as cosmetics, bioengineering, water treatment, biological markers, and targeted drug and gene delivery systems [15,16]. Numerous physicochemical methods are available for the production of metallic NPs, but certain limitations such as toxicity, cost, complexity, and environmental hazards hinder efficacy and consumer acceptance of nanomaterials produced through these methods [15]. Green synthesis of NPs has proved to be the more reliable, cost-effective, and eco-friendly approach mostly employing microorganisms and plants [17]. However, the microbe-mediated synthesis of NPs has gained much attention due to the use of non-toxic reagents and ease in downstream processing [18]. AgNPs fabricated through such green methods have been investigated as antimicrobials and anticancer agents with promising results due to the capping of biomolecules in the interfacial layer [9]. Utilizing bacterial cells as factories to synthesize NPs could be an efficient approach due to less resources utilization of bacteria and ease in downstream processing. Various studies have reported the biosynthesis of AgNPs by using *Bacillus* spp. as cell factories [19–21].

Thus, the current study encompassed the bacterial-mediated synthesis of AgNPs from silver-resistant *B. safensis* strain, isolated from leader industry wastewater, and measurement of antibacterial and anticancer abilities of biogenic AgNPs against two common human pathogens and cancer cell lines.

Materials and methods

Sampling site and isolation of silver-resistant bacteria

Bacterial isolation was based on dilution plate method (Somasegaran and Hoben [22], from a leather industry wastewater contaminated soil sample collected from Kasur, Pakistan (31° 6′ 50 N and 74° 27′ 27 E). Ten isolates were purified by repeated culturing on media plates supplemented with $AgNO_3$ (1 mM). All the isolates were then subjected to tolerate different concentrations (01, 02, 03, 04, 05, 06, 07, 08, 09 and 10 mM) of $AgNO_3$ to measure the minimum inhibitory concentration (MIC) against this salt (Table 1).

Biosynthesis of silver nanoparticles

Based on the maximum silver-resistance ability to isolate TEN12, it was used to synthesize the AgNPs by the intracellular method according to [23]. AgNPs production was investigated at different concentrations of $AgNO_3$ solution (i.e., 0.5, 1, 3, 5, and 7 mM) up to the MIC of the strain. For biosynthesis of AgNPs, *B. safensis* TEN12 culture was grown aerobically in 250 mL Erlenmeyer flask containing nutrient broth medium under shaking conditions (150 rpm) at 28 ± 2 °C for 24 h. An equal volume of different concentrations of $AgNO_3$ was added in 50 mL of over nightly grown bacterial culture in 250 mL flask and incubated again at 28 ± 2 °C and 150 rpm for 24 h. The visual color shift of the reaction from pale yellow to dark brown was the clear indication of reduction of Ag^+ ions to AgNPs. The maximum color change was observed at 5 mM of $AgNO_3$ concentration and thus nanoparticles synthesized at this concentration were used for further studies. Afterward, the reaction mixture was placed in an oven at 60 °C until complete drying followed by grinding to make a fine powder. The powder was washed with ethanol three times by centrifugation at 12,000 *g* for 5 min to remove all the impurities including unreacted silver.

Table 1
Minimum inhibitory concentration (MIC) values of different isolates against $AgNO_3$.

Sr. no	Bacterial strains	MIC (mM)
1	TEN2	2
2	TEN8	4
3	TEN12	7
4	TEN17	2
5	TEN18	5
6	TEN36	3
7	WT6	4
8	WT13	3
9	WT23	3
10	WT42	5

Molecular identification and phylogenetic study

The taxonomic rank of the potent strain TEN12 was identified on a molecular level through *in silico* analyses of 16S rRNA gene sequence. The total genomic DNA of silver-resistant bacterial strain TEN12 was isolated by the CTAB method Wilson [24]. The 16S rRNA gene was amplified using universal primer pair fD1 (5′-AGAGTTTGATCCTGGCTCAG-3′) and rD1 (5′- AAGGAGGTGATC-CAGCC – 3′) as previously described by Weisburg, *et al.* [25]. The amplicon was sequenced using Sanger's sequencing technique from Macrogen, South Korea commercially. The forward and reverse sequences retrieved from Macrogen were analyzed and the final contig was constructed using the online CAP3 assembly software package. The identity of the final sequence was confirmed by comparing it with other sequences present in the databases such as NCBI, EzBioCloud and ribosomal database project (RDP) to confirm the identity of the retrieved sequence. The phylogenetic tree of the 16S rRNA gene sequence of TEN12 and other type strains of genus *Bacillus* constructed with maximum likelihood (ML) method using the MEGA 7.0 software package. The final sequence was deposited in the Genbank of NCBI and accession was obtained.

Characterization of AgNPs

The reaction mixture was scanned using UV–vis spectroscopy (Shimadzu, Kyoto, Japan) to confirm the presence of AgNPs by recording the maximum absorbance (λ_{max}) at a wavelength ranging from 300 to 700 nm at regular time intervals (6, 12, 18 and 24 h) according to Deljou and Goudarzi [26]. FTIR (ATR-FTIR, Bruker, USA) analysis of biogenic AgNPs was used to reveal the functional groups and capping biomolecules responsible for the stability of the AgNPs. For FTIR analysis, the powder form of the biogenic AgNPs was mixed with potassium-bromide (KBr) and spectra were observed by scanning it in the range of 450–4000 cm^{-1} at a resolution of 4 cm^{-1} as demonstrated by Saber, *et al.* [27]. The X-ray diffraction analysis was performed using X-ray diffractometer apparatus (STOE-Germany) with Ag Kα radiations operating at 45 kV voltage and 40 mA of current to analyze the phase conformation and crystalline nature of biogenic AgNPs. Moreover, the average size of the AgNPs was measured by Debye-Scherrer's formula ($D = K\lambda/\beta \cos\theta$). The biogenic AgNPs were further characterized for size, surface morphology and characteristics using SEM (TM-1000, Hitachi, Japan), and TEM (JEM-1230, JEOL, Akishima, Japan) as described by [39]. For SEM analysis, the sample was prepared on the glass slip fixed on the aluminum stub. Before SEM imaging the sample was fixed on the SEM grid by keeping the grid under a mercury lamp for 5 min for drying as reported by Fouad, *et al.* [28]. For TEM analysis, small amount of AgNPs was placed on a carbon-coated copper grid, which subsequently analyzed for morphological characteristics. The EDX analysis was performed for the confirmation of metallic fractions in biogenic AgNPs. The biogenic AgNPs were analyzed through SEM, TEM, and EDX at Electron Microscopy Center of Zhejiang University, China.

Antibacterial activity of AgNPs

Antimicrobial activity of biogenic AgNPs was evaluated by using agar well-diffusion assay as described by Elbeshehy, *et al.* [29]. The human pathogenic bacteria *S. aureus* ATCC25923 and *E. coli* ATCC25922 were grown in nutrient broth (1×10^8 CFU mL^{-1}) at 37 °C for 24 h and swabbed uniformly on Muller Hinton agar (MHA) media plates using a sterile cotton swab. The plates were subjected to the formation of five wells, each of 5 mm diameter, with the help of sterile borer. A volume of 20 μl of four different concentrations (*viz.*, 5, 10, 15, and 20 μg mL^{-1}) of AgNPs suspensions were poured into the corresponding wells. The well supplied with the same volume of sterile deionized distilled water was used as a control to assess the comparative antimicrobial activity. The experiment was conducted in triplicate in order to achieve maximum experimental accuracy. After the incubation period, the diameters of inhibition zones were measured edge to edge across the center of the disk.

The minimum inhibitory concentration (MIC) of the biogenic AgNPs against *S. aureus* and *E. coli* strains was determined in 96-well microtiter plates (Corning-Costar Corp., Corning, NY, USA) using micro dilution method according to Ibrahim *et al.* [39]. The human pathogenic bacteria were grown aerobically in the LB-broth medium at 37 °C and 150 rpm for 24 h and the cell density was adjusted to 10^8 CFU mL^{-1}. A volume of 200 μl of LB-broth medium was added into the wells of microtiter plates containing 10 μl of bacterial culture and 20 μl four different concentrations of AgNPs suspensions (*viz.*, 5, 10, 15, and 20 μg mL^{-1}). LB broth medium serving as negative control received only the broth and sterile distilled water, while pathogen culture without AgNPs was the positive control and received 20 μl of sterile distilled water. The 96 wells plates were then placed in an incubator at 37 °C for 48 h under constant shaking of 200 rpm. For MIC evaluation, the plates were scanned for absorbance at the wavelength of 600 nm using a scanning microplate spectrophotometer (Thermo Fisher Scientific Inc., Waltham, MA, USA). The experiment was run with six replications and the absorbance values measured in wells with bacterial cultures were normalized with the values of negative control.

Anticancer activity (MTT assay)

Human hepatic (HepG2) cancer cell line and Human embryonic kidney (HEK293) normal cell line were maintained in Dulbecco's modified Eagle's medium (DMEM) with gultaMAX supplemented with 10% fetal bovine serum (FBS) (Gibco), at 37 ℃ in a humidified atmosphere containing 5% CO2. Human hepatic carcinoma cell line (HepG2) was used to study the anticancer activities of AgNps whereas non-cancerous cell line human embryonic kidney (HEK293) was used as control to identify the selectivity of AgNPs. To study the putative cytotoxic effects, cells were seeded in 96-cell culture plate at an initial concentration of 1×10^5 cells/well and were incubated under the above-described conditions. Cells were treated with 20 μl of four different concentrations (5, 10, 15, and 20 μg mL^{-1}) of AgNPs and the same volume of phosphate buffer saline (PBS) as control. The plates after treatment were incubated for 48h in order to perform MTT assay according to [30]. The MTT was prepared by dissolving 3-(4,5-dimethylthiazol-2-yl)-2,5-diphenyl tetrazolium bromide at a concentration of 5 mg mL^{-1} in PBS. After 48h of incubation, 10 μl of MTT solution was added to each well and the plates were incubated for 4h. The purple color crystals formed were dissolved in 150 μl dimethyl sulphoxide (DMSO). The optical density (OD) was measured at 490 nm wavelength in a multi-well ELISA plate reader (Bio Tek Instruments, Inc, USA).

Observation of cell morphology

To investigate the effects of different concentrations of AgNPs suspensions on the morphology of HepG2 cells, the cells were seeded in a 12-well cell culture plate at a concentration of 1×10^5 cells/well and incubated at 37 ℃ in a humidified atmosphere containing 5% CO_2. Cells were treated with the above-mentioned concentrations (5, 10, 15, and 20 μg mL^{-1}) of AgNPs suspension by adding 20 μl volume of each concentration. The

plates after treatment were incubated for 24 h and cell morphology was examined under the phase-contrast inverted biological microscope (MEIJI TC5200, USA) after incubation.

Statistical analysis

The statistical analysis of data was performed using one way analysis of variance using GraphPad Prism software (version 8.0). The Fisher's LSD test was performed to determine the least significant differences among treatment means with probability level 95% (*), 99% (**) and 99.9% (***).

Results and discussion

Selection and taxonomic identification of the strain TEN12

Our 10 isolates, TEN12 was selected for the bioengineering of AgNPs based on its maximum tolerance to $AgNO_3$. The 16S rRNA gene sequence of the strain TEN12 showed 99.89% similarity with *Bacillus safensis* NBRC 100,820 (NR_113945). Further, the sequence was found 99.89% similar to the *Bacillus safensis* subsp. *safensis* FO-36b^T (ASJD01000027) in EzBioCloud database and the sequence was found similar to *Bacillus safensis* SAFN-037 (AY167880) in the RDP database. In the phylogenetic tree, the strain TEN12 formed a cluster with *Bacillus safensis* subsp. *osmophilus* BC09^T (KY990920) and *Bacillus safensis* subsp. *safensis* FO-36b^T (ASJD01000027) (Fig. 1). These results confirmed the taxonomic rank of the TEN12 strain as *Bacillus safensis* and hence named as '*Bacillus safensis* TEN12 (Accession no. MN121588).

Biosynthesis and characterization of AgNPs

Biogenic AgNPs were synthesized intracellularly by using the *B. safensis* TEN12 and maximum color change from pale yellow to reddish-brown was observed at 5 mM $AgNO_3$ concentration after 24 h due to excitation of surface plasmon vibrations [31]. This indicated that there might be some inherent physiological and genetic mechanisms involved in metal-tolerant bacteria for NP biosynthesis. Earlier studies have been reported the use of *Bacillus* spp. for AgNPs biosynthesis, however, a thorough insight into the metabolic role of silver resistance in the bacterial synthesis of NPs is necessary [32,33]. The bioprospecting of *Bacillus* sp. for AgNPs production has been previously reported by Deljou and Goudarzi [26], who synthesized spherical-shaped AgNPs with size ranging from 7 to 31 nm by using $AgNO_3$ as precursor salt. In contrast, this study firstly reported that *B. safensis* TEN12 exhibited strong resistance to $AgNO_3$. The unique feature makes this bacterium a prospective candidate for biosynthesis and application of silver nanoparticles. Moreover, the biological synthesis of AgNPs has distinct advantages over chemical synthesis in terms of less resource utilization and environmental safety due to the low by-product accumulation and disposal. It is also believed that the biogenic NPs are more stable as compared to chemically-synthesized ones due to the strong capping of functional groups in the interfacial layer [34].

The UV–vis spectra with a strong absorption peak at 426.18 nm after 24 h further confirmed the production of AgNPs in the reaction mixture. The synthesis of the AgNPs was confirmed at four different time intervals and no further increase was observed after 24 h (Fig. 2). The results of UV–vis analysis were found in line with Omole, *et al.* [35], who reported a strong peak at 390 nm by using the culture supernatant of *B. subtilis* at 1 mM $AgNO_3$ concentration, however, the current study confirmed the biosynthesis of AgNPs at at 5 mM concentration of $AgNO_3$.

The FTIR analysis confirmed the presence of bacteria-oriented functional groups over the surface of nanoparticles. The FTIR analysis of biogenic AgNPs produced from *B. safensis* TEN12 showed strong absorption spectra at 3427.84 cm^{-1}, 2929.99 cm^{-1}, 1637.03 cm^{-1}, 1392.11 cm^{-1} and 1104.68 cm^{-1} (Fig. 3). The presence of alcoholic hydroxyl (O-H) group and C-H stretching group of alkanes over the surface of AgNPs was confirmed by strong peaks at 3427.84 cm^{-1} and 2929.99 cm^{-1} in FTIR spectra (Fig. 4). The absorption peaks at 1637.03 cm^{-1} and 1392.11 cm^{-1} were due to the C = C stretching group of alkene and N-O stretching group of nitro compound respectively, whereas, the bending of O-H group and stretching of C-N group of amine showed absorption spectra at 1104.68 cm^{-1}. Similarly, Majeed, Danish, Zahrudin and Dash [30], concluded that the capping proteins prevent the nanomaterials from oxidation and deterioration that subsequently helped in the long-term stabilization of nanoparticles. In addition, AgNPs

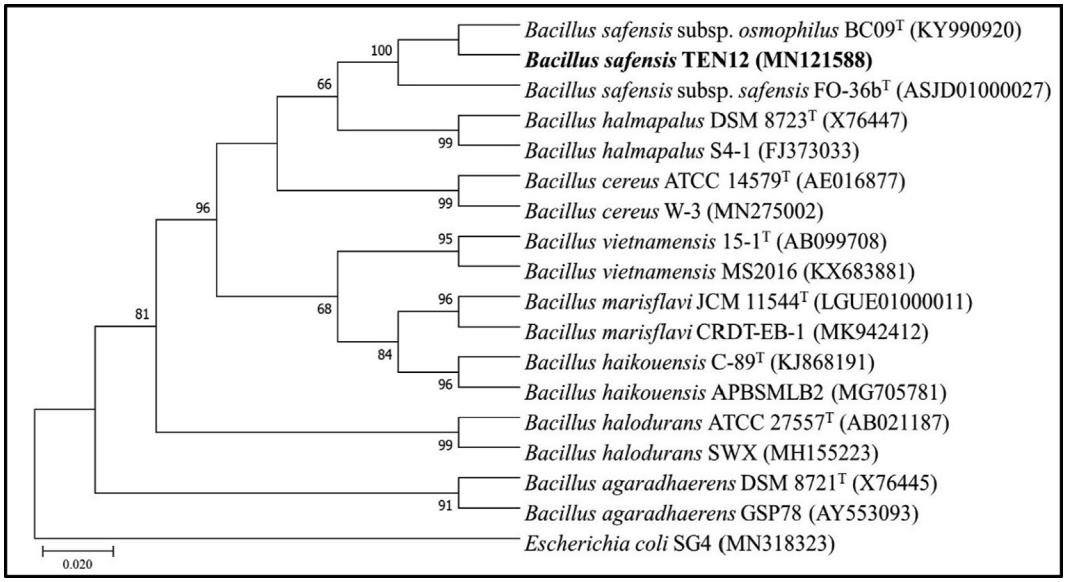

Fig. 1. Phylogenetic tree of *B. safensis* TEN12 with the type strains and closest GenBank matches of genus Bacillus. The evolutionary history was inferred using the Maximum Likelihood (ML) method. The percentages (≥50%) of replicate trees in which the associated taxa clustered together in the bootstrap test (1000 replicates) are shown. The evolutionary distances were computed using the Tamura-Nei model and are in the units of the number of base substitutions per site (represented at the bottom of the tree).

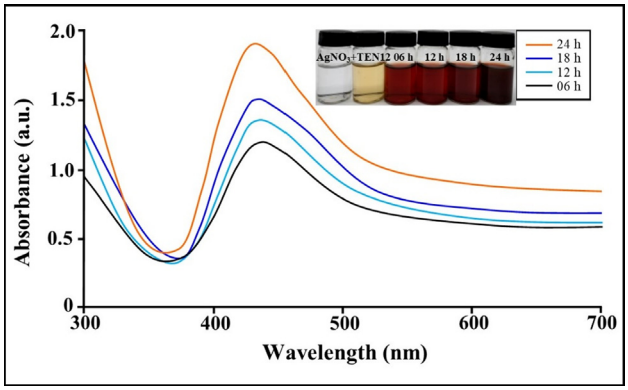

Fig. 2. UV–vis spectrum of bacterial culture containing biogenic AgNPs from *B. safensis* TEN12 after at different time intervals. The absorption-spectrum of biogenic AgNPs showed a strong peak at 426.18 nm after 24 h.

fabricated through green methods are comparatively more stable than the chemically-produced NPs, adding more significance in terms of their application as antimicrobials and anticancer agents [36,37].

The X-ray diffraction data of AgNPs produced from *B. safensis* TEN12 showed characteristic diffraction peaks at 27.19°, 31.52°, 37.93°, 45.26°, 56.30°, 75.17° which were corresponding to 111, 200, 220, 222, 400, 420 planes, respectively (Fig. 3), of cubic silver. These diffraction planes were in agreement JCPDS data for AgNPs (JCPDS card #: 04–0783) which revealed the crystallinity of AgNPs [38]. The average particle size of biogenic AgNPs measured using Debye-Sherrer's equation was found to be 27.78 nm. Similar results have been previously described by Kalishwaralal, *et al.* [39], who reported the production of AgNPs by silver-resistant *B. licheniformis* with similar diffraction peaks 111, 200, 220, and 311. SEM, TEM, and EDX analysis provided the size and surface morphology details of biogenic AgNPs synthesized from *B. safensis* TEN12. SEM and TEM analysis revealed that the biogenic AgNPs have a spherical shape with the particle size ranging from 22.77 to 45.98 nm (Fig. 4). Ibrahim, *et al.* [40], obtained similar results of AgNPs with spherical shape and size ranging from 25 to 50 nm using the culture supernatant of *B. siamensis*. The elemental profile analyzed using EDX revealed that the biogenic AgNPs in addition to Ag (93.54%) also contain 3.67, 1.91 and 0.81% of chlorine (Cl), copper (Cu) and sulfur (S) respectively (Fig. 4c). Hossain, *et al.* [41], previously reported that the

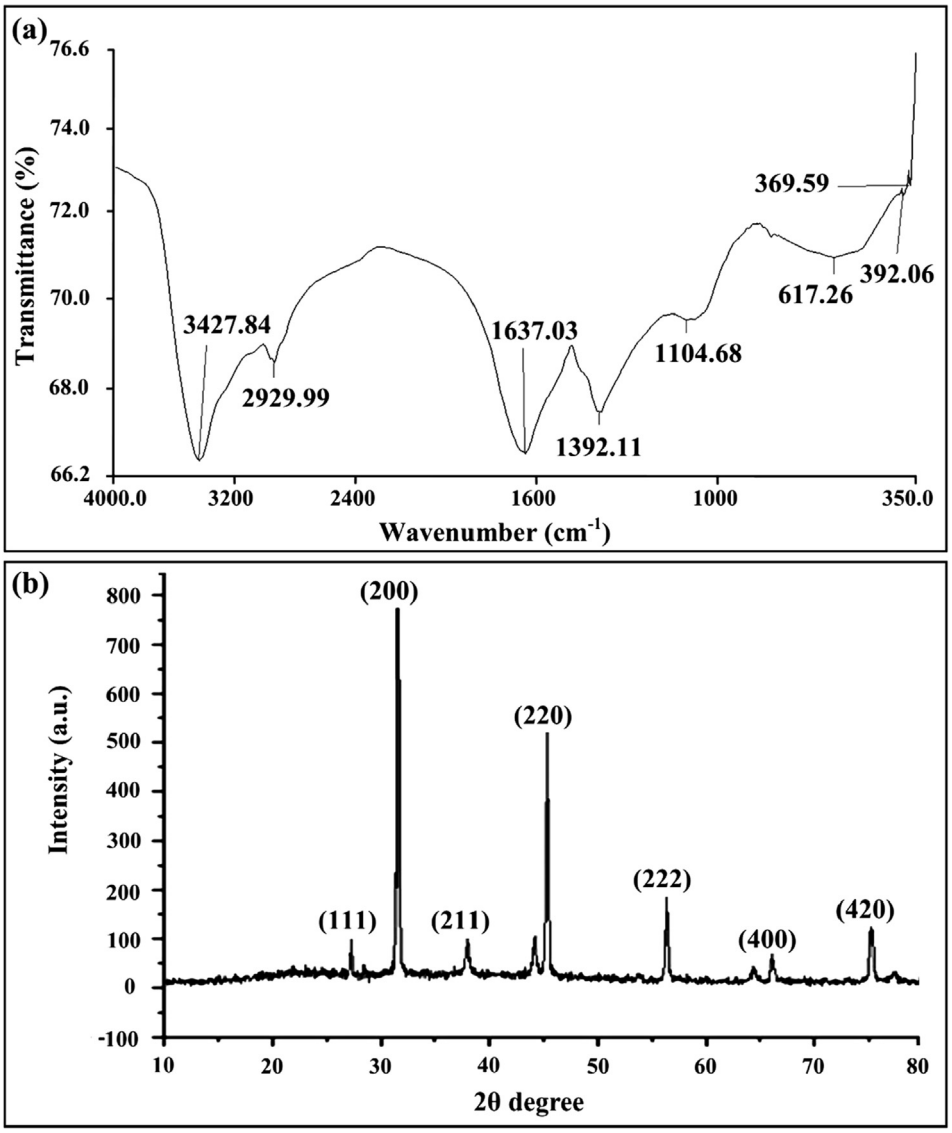

Fig. 3. Characterization of the biogenic AgNPs synthesized from *B. safensis* TEN12 (a) FTIR spectra of the biogenic AgNPsin the wavelength range of 350–4000 cm-1 (b) XRD spectrum of biogenic AgNPs.

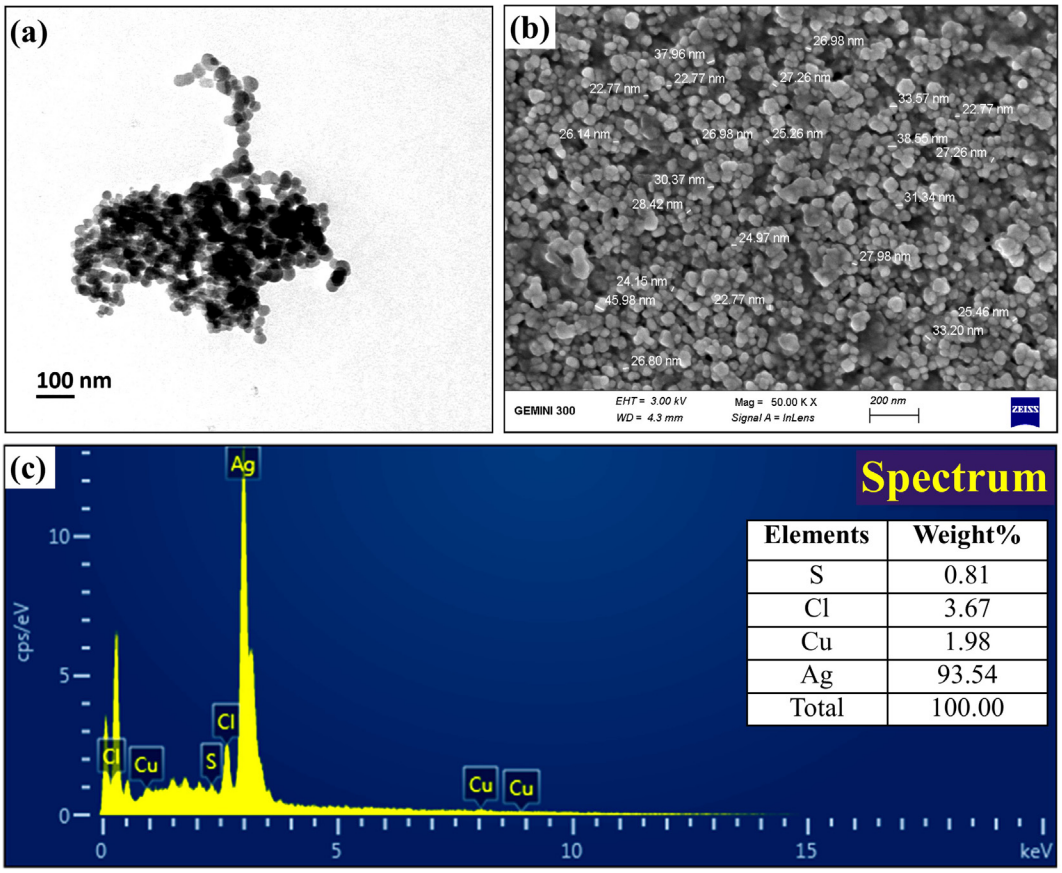

Fig. 4. Imaging of the biogenic AgNPs synthesized from *B. safensis* TEN12 (a) Transmission electron microscopy (b) Scanning electron microscopy (C) EDX spectrum.

AgNPs showed an absorption peak of the silver element at about 3 KeV and the wt% of silver and chlorine elements were about 83.1 and 16.1% respectively.

Antibacterial activity of AgNPs

The antibacterial potential of biogenic AgNPs is well-established in the literature due to their unique properties such as disruption of cell membranes and cell walls, interrupted ATP production, and blockage of cell transport and replication. Various studies reported that biogenic AgNPs effectively controlled the human pathogenic bacteria *S. aureus* and *E. coli in vitro* [42,43]. The antibacterial activity results of AgNPs significantly suppressed the growth of human pathogens *S. aureus* and *E. coli* as compared to the non-treated control. In current study, the diameters of zone of inhibition were found to be (13.16, 16.92, 17.01 and 20.35 mm) at four varying concentrations of AgNPs (5, 10, 15, and 20 μg mL^{-1}) respectively against *S. aureus*, whereas, for *E. coli* AgNPs showed diameters of zone of inhibition as 12.83 mm at 5 μg mL^{-1} concentration, 13.42 mm at 10 μg mL^{-1} concentration, 17.69 mm at 15 μg mL^{-1} concentration and 19.69 mm at 20 μg mL^{-1} concentration. The highest concentration (i.e., 20 μg mL^{-1}) of AgNPs showed the maximum diameter of the zone of inhibition (Fig. 5). Similar results have been reported by Majeed, Danish, Zahrudin and Dash [30], who observed the zone of inhibition (17 and 16 mm) against *E. coli* and *S. aureus* respectively, at 20 μg mL^{-1} concentration of AgNPs.

In vitro MIC results indicated that the AgNPs significantly inhibited the growth of *S. aureus* and *E. coli* after incubation of 48 h. The four varying concentrations of AgNPs suspension (5, 10, 15, and 20 μg mL^{-1}) caused (12.65, 32.91, 56.54, 78.48%) reduction of *S. aureus* respectively, and (38.50, 45.98, 63.63, 75.40%) reduction against *E. coli* at OD600, respectively (Fig. 5). Similarly, Velmurugan, *et al.* [44], reported that the AgNPs possess the lowest MIC against *S. aureus* and *P. fluorescens* as compared with control. Earlier studies have suggested that the antibacterial effect of AgNPs on the pathogenic bacteria might be due to the destructive effect of different functional groups capping the NPs which support the stabilization and binding with the bacterial surface. These biogenic AgNPs are known to alter the bacterial cell permeability, disturbing cellular respiration and induce damage by reacting with proteins and DNA [45,46]. Therefore, the present study, as well as the previous literature highlights the starring potential of biogenic AgNPs in the control of human pathogenic bacteria.

Cell viability and anticancer activity of AgNPs

The effect of AgNPs on the viability of the cancer HepG2 cell line and a normal HEK293 cell line with different concentrations of AgNPs suspension was observed using MTT assay. Sivamaruthi, *et al.* [47], previously revealed the toxic effect of AgNPs against human lung cancer A549 cell line under *in vitro* conditions. The results of our study revealed that the viability of the cancer HepG2 cell line was 84.42, 65.25, 48.76 and 36.25%, respectively, at 5, 10, 15 and 20 μg mL^{-1} AgNPs concentrations (Fig. 6). Whereas, AgNPs have no cytotoxic effect on normal HEK293 cell line (Fig. 7).

Hence, our results revealed the significant anticancer activity and cell viability of HepG2 significantly decreased with increasing the dose of biogenic AgNPs as compared to the non-treated control. Further, the effects of different AgNPs concentrations on the normal human renal cell line suggested that AgNPs have no cytotoxic effect on normal cells and can kill cancerous cells in a targeted manner. Similar results have been reported by Kahsay,

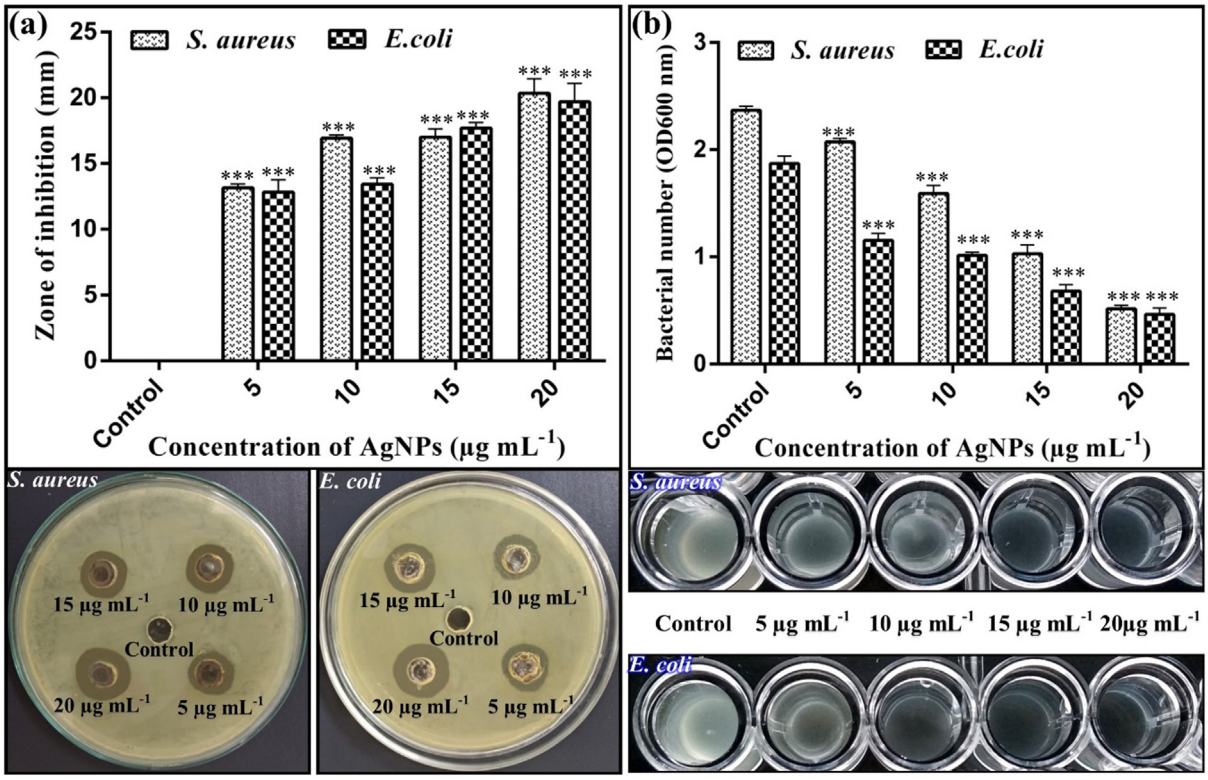

Fig. 5. Concentration-dependent antibacterial activity of AgNPs against *S. aureus* and *E. coli*.

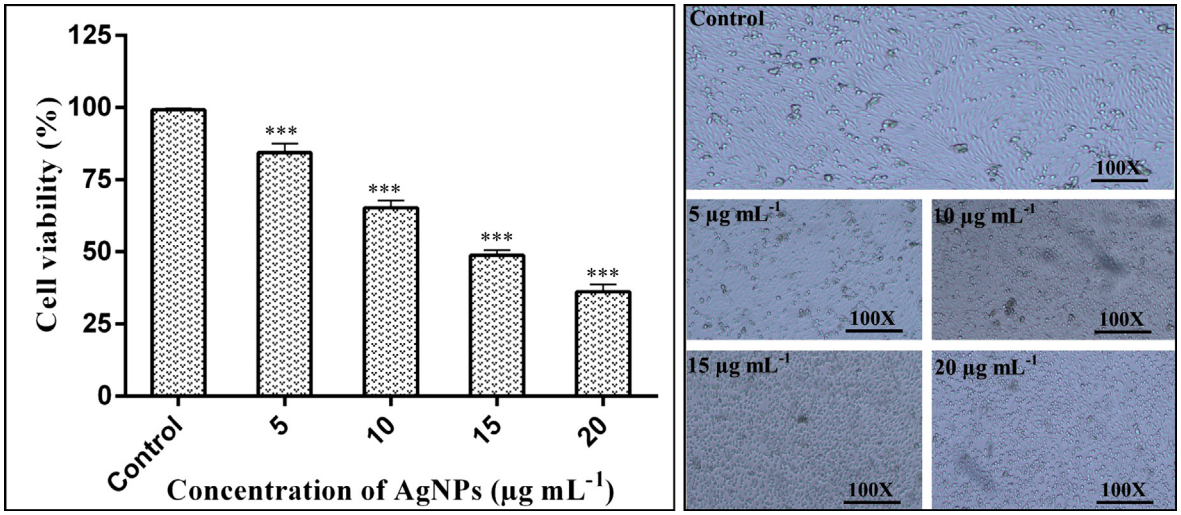

Fig. 6. Anticancer activity of AgNPs in various concentrations against the human hepatic (HepG2) cancer cell line. Morphological changes images were taken using an inverted phase-contrast microscope at 100X magnification.

RamaDevi, Kumar, Mohan, Tadesse, Battu and Basavaiah [15], who observed the cytotoxic effect of AgNPs against HepG2. Their results revealed that AgNPs significantly inhibited the proliferation of human liver cancer HepG2 cell lines by inducing apoptosis and reducing DNA synthesis in cancer cells. The studies have also shown that AgNPs can pass through biological barriers of cells and interact with cell components that leads to the production of reactive oxygen species (ROS) and in turn reducing antioxidant capicities and causing apoptosis in cancer cells [48,49]. In addition, AgNPs have shown to restrict angiogenesis: an essencial step in tumor growth [50]. However, insufficient literature has been available until now about the AgNPs-induced toxicity mechanism and their effect on the normal human cell line. The functional groups of intracellular proteins coated on AgNPs might be involved in cytotoxicity and the killing of cancerous cells [51]. However, according to Xue, *et al.* [52], the cytotoxicity of AgNPs against HepG2 cell line has a positive correlation with the concentration of AgNPs. The direct contact of AgNPs with HepG2 cells may bring an increase in cytotoxicity, generation of reactive oxygen species (ROS), induction of apoptosis, and mitochondrial injury, which may increase the cellular oxidative stress that leads to killing of cancerous cells.

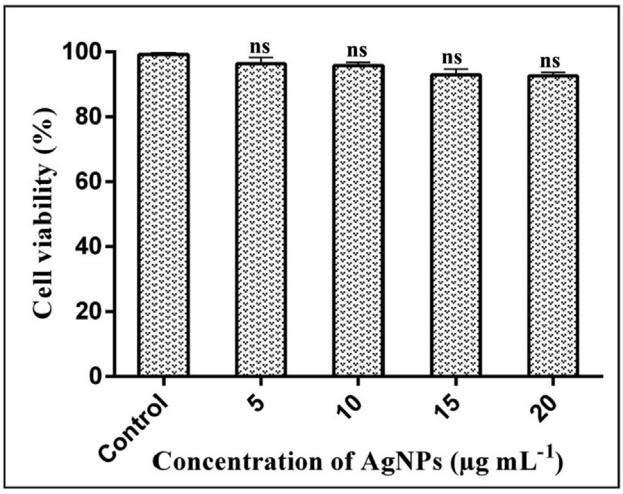

Fig. 7. Anticancer activity of AgNPs in various concentrations against the human embryonic kidney (HEK293) normal cell line.

Morphological analysis of HepG2

The cells in the control group appeared in normal morphology and were attached to the surface whereas the cells treated with AgNPs suspensions lost their normal shape and cell adhesion capacity to the surface and were shrunken and decreased the cell density. The similar kind of changes in the morphology of different cancer cells treated AgNPs have already been reported Al-Sheddi, Farshori, Al-Oqail, Al-Massarani, Saquib, Wahab, Musarrat, Al-Khedhairy and Siddiqui [34]. The change in the morphology of cells might be due to the fact that AgNPs and associated capping groups after penetrating the cells stimulate the necrosis mechanism to induce cytotoxicity [53].

Conclusion

The supernatant of Ag-resistant *B. safensis* TEN12 was used for the intracellular biosynthesis of AgNPs. The UV–vis spectroscopy and FTIR analysis revealed the production of AgNPs stabilized by the alcoholic group and capping proteins. Moreover, XRD, SEM, TEM, and EDX analysis revealed that the biogenic AgNPs were present in a spherical shape with an average particle size ranging from 22.77 to 45.98 nm. AgNPs showed potential bacteriocidal effect against human pathogenic bacteria *S. aureus* and *E. coli* and anticancer activity against cancer cell line HepG2. The biological synthesis of AgNPs possessing antibacterial and anticancer activity will help to develop a symbiotic association between medical science and nanoscience to control the fatal diseases in a more efficient way. However, future investigations are needed to evaluate the effect of biogenic AgNPs on the beneficial microbiota and normal cells as well as animal trials for their large-scale applications.

Declaration of Competing Interest

The authors declare that they have no known competing financial interests or personal relationships that could have appeared to influence the work reported in this paper.

Acknowledgments

The authors express gratitude to Dr. Mahmood Ahmed, Mr. Fahd Shahzad, Ms. Zahra Aslam and Ms. Noor Fatima for technical assistance and English editing.

Funding

This research work has been partially supported by PhosAgro/UNESCO/IUPAC research grant # 82 and the annual research grant of the Department of Bioinformatics and Biotechnology, Government College University, Faisalabad.

References

[1] Abdel-Aziz MM, Elella MHA, Mohamed RR. Green synthesis of quaternized chitosan/silver nanocomposites for targeting mycobacterium tuberculosis and lung carcinoma cells (A-549). Int J Biol Macromol 2020;142:244–53.
[2] Kim S-H, Lee H-S, Ryu D-S, Choi S-J, Lee D-S. Antibacterial activity of silver-nanoparticles against *Staphylococcus aureus* and *Escherichia coli*. Korean J Microbiol Biotechnol 2011;39:77–85.
[3] Kobayashi SD, DeLeo FR. Towards a monoclonal antibody-based therapy for prevention and treatment of *Staphylococcus aureus* infections. Oxford University Press US; 2018.
[4] DeLeo FR, Otto M, Kreiswirth BN, Chambers HF. Community-associated meticillin-resistant Staphylococcus aureus. The Lancet 2010;375:1557–68.
[5] Boswihi SS, Udo EE. Methicillin-resistant *Staphylococcus aureus*: An update on the epidemiology, treatment options and infection control. Current Medicine Research and Practice 2018;8:18–24.
[6] Mellata M, Johnson JR, Curtiss III R. *Escherichia coli* isolates from commercial chicken meat and eggs cause sepsis, meningitis and urinary tract infection in rodent models of human infections. Zoonoses Public Hlth 2018;65:103–13.
[7] Jang J, Hur HG, Sadowsky MJ, Byappanahalli M, Yan T, Ishii S. Environmental *Escherichia coli*: ecology and public health implications-a review. J Appl Microbiol 2017;123:570–81.
[8] Monowar T, Rahman M, Bhore S, Raju G, Sathasivam K. Silver Nanoparticles Synthesized by Using the Endophytic Bacterium *Pantoea ananatis* are Promising Antimicrobial Agents against Multidrug Resistant Bacteria. Molecules 2018;23:3220.
[9] Rajeshkumar S, Malarkodi C, Vanaja M, Annadurai G. Anticancer and enhanced antimicrobial activity of biosynthesizd silver nanoparticles against clinical pathogens. JMoSt 2016;1116:165–73.
[10] Ozakyol A. Global epidemiology of hepatocellular carcinoma (HCC epidemiology). J. Gastrointest. Cancer 2017;48:238–40.
[11] Petrick JL, Kelly SP, Altekruse SF, McGlynn KA, Rosenberg PS. Future of hepatocellular carcinoma incidence in the United States forecast through 2030. J Clin Oncol 2016;34:1787.
[12] Massarweh NN, El-Serag HB. Epidemiology of hepatocellular carcinoma and intrahepatic cholangiocarcinoma. Cancer Control 2017;24. 1073274817729245.
[13] Janib SM, Moses AS, MacKay JA. Imaging and drug delivery using theranostic nanoparticles. Adv Drug Del Rev 2010;62:1052–63.
[14] Madheswaran T, Kandasamy M, Bose RJ, Karuppagounder V. Current potential and challenges in the advances of liquid crystalline nanoparticles as drug delivery systems. Drug Discovery Today 2019.
[15] Kahsay MH, RamaDevi D, Kumar YP, Mohan BS, Tadesse A, Battu G, Basavaiah K. Synthesis of silver nanoparticles using aqueous extract of Dolichos lablab for reduction of 4-Nitrophenol, antimicrobial and anticancer activities. OpenNano 2018;3:28–37.
[16] Singh R. Nalwa, HS Medical applications of nanoparticles in biological imaging, cell labeling, antimicrobial agents, and anticancer nanodrugs. J Biomed Nanotechnol 2011;7:489–503.
[17] Zhang X, Yan S, Tyagi R, Surampalli R. Synthesis of nanoparticles by microorganisms and their application in enhancing microbiological reaction rates. Chemosphere 2011;82:489–94.
[18] Dakhil AS. Biosynthesis of silver nanoparticle (AgNPs) using *Lactobacillus* and their effects on oxidative stress biomarkers in rats. Journal of King Saud University-Science 2017;29:462–7.
[19] Silambarasan S, Abraham J. Biosynthesis of silver nanoparticles using the bacteria *Bacillus cereus* and their antimicrobial property. Int J Pharm Pharm Sci 2012;4:536–40.
[20] Das VL, Thomas R, Varghese RT, Soniya E, Mathew J, Radhakrishnan E. Extracellular synthesis of silver nanoparticles by the *Bacillus* strain CS 11 isolated from industrialized area. 3. Biotech 2014;4:121–6.
[21] Khaleghi M, Khorrami S, Ravan H. Identification of *Bacillus thuringiensis* bacterial strain isolated from the mine soil as a robust agent in the biosynthesis of silver nanoparticles with strong antibacterial and anti-biofilm activities. Biocat Agricul Biotechnol 2019;18:101047.
[22] Somasegaran P, Hoben HJ. Handbook for rhizobia: methods in legume-Rhizobium technology. Springer Science & Business Media; 2012.
[23] Otari S, Patil R, Ghosh S, Thorat N, Pawar S. Intracellular synthesis of silver nanoparticle by actinobacteria and its antimicrobial activity. Spectrochim Acta Part A Mol Biomol Spectrosc 2015;136:1175–80.
[24] Wilson K. Preparation of genomic DNA from bacteria. Curr Protoc Mol Biol 2001;56(2). pp. 4. 1–2.4. 5.
[25] Weisburg WG, Barns SM, Pelletier DA, Lane DJ. 16S ribosomal DNA amplification for phylogenetic study. J Bacteriol 1991;173:697–703.

[26] Deljou A, Goudarzi S. Green extracellular synthesis of the silver nanoparticles using *thermophilic Bacillus* sp. AZ1 and its antimicrobial activity against several human pathogenetic bacteria. Iran. J Biotechnol 2016;14:25.
[27] Saber MM, Mirtajani SB, Karimzadeh K. Green synthesis of silver nanoparticles using Trapa natans extract and their anticancer activity against A431 human skin cancer cells. J Drug Deliv Sci Technol 2018;47:375–9.
[28] Fouad H, Hongjie L, Yanmei D, Baoting Y, El-Shakh A, Abbas G. Jianchu, M Synthesis and characterization of silver nanoparticles using *Bacillus amyloliquefaciens* and Bacillus subtilis to control filarial vector Culex pipiens pallens and its antimicrobial activity. Artif Cell Nanomed Biotecnol 2017;45:1369–78.
[29] Elbeshehy EK, Elazzazy AM, Aggelis G. Silver nanoparticles synthesis mediated by new isolates of Bacillus spp., nanoparticle characterization and their activity against Bean Yellow Mosaic Virus and human pathogens. Front Microbiol 2015;6:453.
[30] Majeed S, Danish M, Zahrudin AHB, Dash GK. Biosynthesis and characterization of silver nanoparticles from fungal species and its antibacterial and anticancer effect. K Int J Mod Sci 2018;4:86–92.
[31] Ingle A, Gade A, Pierrat S, Sonnichsen C, Rai M. Mycosynthesis of silver nanoparticles using the fungus *Fusarium acuminatum* and its activity against some human pathogenic bacteria. Curr Nanosci 2008;4:141–4.
[32] Banu AN, Balasubramanian C, Moorthi PV. Biosynthesis of silver nanoparticles using *Bacillus thuringiensis* against dengue vector, Aedes aegypti (Diptera: Culicidae). Parasitol Res 2014;113:311–6.
[33] Ghiuță I, Cristea D, Croitoru C, Kost J, Wenkert R, Vyrides I, et al. Characterization and antimicrobial activity of silver nanoparticles, biosynthesized using *Bacillus* species. ApSS 2018;438:66–73.
[34] Al-Sheddi ES, Farshori NN, Al-Oqail MM, Al-Massarani SM, Saquib Q, Wahab R, et al. Anticancer Potential of Green Synthesized Silver Nanoparticles Using Extract of Nepeta deflersiana against Human Cervical Cancer Cells (HeLA). Bioinorg Chem Appl 2018;2018.
[35] Omole R, Torimiro N, Alayande S, Ajenifuja E. Silver nanoparticles synthesized from *Bacillus subtilis* for detection of deterioration in the post-harvest spoilage of fruit. Sustain Chem Pharm 2018;10:33–40.
[36] Patil MP, Kim G-D. Eco-friendly approach for nanoparticles synthesis and mechanism behind antibacterial activity of silver and anticancer activity of gold nanoparticles. Appl Microbiol Biotechnol 2017;101:79–92.
[37] Singh G, Babele PK, Shahi SK, Sinha RP, Tyagi MB, Kumar A. Green synthesis of silver nanoparticles using cell extracts of Anabaena doliolum and screening of its antibacterial and antitumor activity. J Microbiol Biotechnol 2014;24:1354–67.
[38] John T, Parmar KA, Tak P. Biosynthesis and Characterization of Silver Nanoparticles from Tinospora cordifolia Root Extract. J Nanosci Technol 2019:622–6.
[39] Kalishwaralal K, Deepak V, Ramkumarpandian S, Nellaiah H, Sangiliyandi G. Extracellular biosynthesis of silver nanoparticles by the culture supernatant of *Bacillus licheniformis*. MatL 2008;62:4411–3.
[40] Ibrahim E, Fouad H, Zhang M, Zhang Y, Qiu W, Yan C, et al. Biosynthesis of silver nanoparticles using endophytic bacteria and their role in inhibition of rice pathogenic bacteria and plant growth promotion. RSC Adv 2019;9:29293–9.
[41] Hossain A, Hong X, Ibrahim E, Li B, Sun G, Meng Y, et al. Green Synthesis of Silver Nanoparticles with Culture Supernatant of a Bacterium *Pseudomonas rhodesiae* and Their Antibacterial Activity against Soft Rot Pathogen Dickeya dadantii. Molecules 2019;24:2303.
[42] Saravanan M, Barik SK, MubarakAli D, Prakash P, Pugazhendhi A. Synthesis of silver nanoparticles from *Bacillus brevis* (NCIM 2533) and their antibacterial activity against pathogenic bacteria. Microb Pathog 2018;116:221–6.
[43] Munteanu D. Characterization and antimicrobial activity of silver nanoparticles, biosynthesized using. *Bacillus* species 2017.
[44] Velmurugan P, Iydroose M, Mohideen MHAK, Mohan TS, Cho M. Biosynthesis of silver nanoparticles using *Bacillus subtilis* EWP-46 cell-free extract and evaluation of its antibacterial activity. Bioprocess Biosystems Eng 2014;37:1527–34.
[45] Durán N, Durán M, de Jesus MB, Seabra AB, Fávaro WJ, et al. Silver nanoparticles: A new view on mechanistic aspects on antimicrobial activity. Nanomed Nanotechnol Biol Med 2016;12:789–99.
[46] Hamouda RA, Hussein MH, Abo-elmagd RA, Bawazir SS. Synthesis and biological characterization of silver nanoparticles derived from the cyanobacterium *Oscillatoria limnetica*. Sci Rep 2019;9:1–17.
[47] Sivamaruthi BS, Ramkumar VS, Archunan G, Chaiyasut C, Suganthy N. Biogenic synthesis of silver palladium bimetallic nanoparticles from fruit extract of Terminalia chebula–In vitro evaluation of anticancer and antimicrobial activity. J Drug Deliv Sci Technol 2019;51:139–51.
[48] Kruszewski M, Brzoska K, Brunborg G, Asare N, Dobrzyńska M, Dušinská M, et al. Toxicity of silver nanomaterials in higher eukaryotes. Advances in molecular toxicology, Elsevier 2011;5:179–218.
[49] Bartlomiejczyk T, Lankoff A, Kruszewski M, Szumiel I. Silver nanoparticles–allies or adversaries?. Ann Agr Env Med 2013, 20..
[50] Gurunathan S, Lee KJ, Kalishwaralal K, Sheikpranbabu S, Vaidyanathan R, Eom SH. Antiangiogenic properties of silver nanoparticles. Biomaterials 2009;30:6341–50.
[51] Jeyaraj M, Rajesh M, Arun R, MubarakAli D, Sathishkumar G, Sivanandhan G, et al. An investigation on the cytotoxicity and caspase-mediated apoptotic effect of biologically synthesized silver nanoparticles using Podophyllum hexandrum on human cervical carcinoma cells. Colloids Surf B Biointerfaces 2013;102:708–17.
[52] Xue Y, Zhang T, Zhang B, Gong F, Huang Y, Tang M. Cytotoxicity and apoptosis induced by silver nanoparticles in human liver HepG2 cells in different dispersion media. J Appl Toxicol 2016;36:352–60.
[53] AshaRani P, Low Kah Mun G, Hande MP, Valiyaveettil S. Cytotoxicity and genotoxicity of silver nanoparticles in human cells. ACS Nano 2008;3:279–90.